International Journal of Mass Spectrometry 436 (2019) 25–32

Contents lists available at ScienceDirect

International Journal of Mass Spectrometry

journal homepage: www.elsevier.com/locate/ijms

Full Length Article

Residue-specific radical-driven dissociation of peptides using matrix-assisted laser desorption/ionization in-source decay with hydrogen-donating and -abstracting matrices

Keishiro Nagoshi, Mitsuo Takayama *

Mass Spectrometry Laboratory, Graduate School in Nanobioscience, Yokohama City University, 22-2 Seto, Kanazawa-ku, Yokohama 236-0027, Japan

ARTICLE INFO

Article history:
Received 24 May 2018
Accepted 1 November 2018
Available online 19 November 2018

dedicated to Professor Shuying Liu in honor of her 75th birthday.

Keywords:
MALDI
In-source decay
Radical-driven dissociation
Hydrogen-excess/deficient peptides
Residue-specific cleavage

ABSTRACT

Radical-driven dissociation (RDD) of peptides was examined by MALDI-ISD with hydrogen-donating and -abstracting matrices. The observed fragment ions could be explained by the RDD of carbonyl-carbon (C_{CO})-centered hydrogen-excess radical ions $[M + H_{CO} + H]^{\cdot+}$ and β-carbon (Cβ)-centered hydrogen-deficient radical ions $[M - H\beta + H]^{\cdot+}$. The ISD spectra with hydrogen-abstracting and -donating matrices yielded C-terminal $[x]^+$, $[y]^+$ and $[z]^+$ ions and C-terminal $[x + 2H]^+$, $[y + 2H]^+$ and $[z + 2H]^+$ ions, respectively, indicating the formation of MALDI plume devoid or rich in hydrogen radicals H·. The residue-specific cleavages of the hydrogen-deficient radical ions $[M-H+H]^{\cdot+}$ gave $[d]^+$ ions for Asp and Met, $[b]^+$, $[y]^+$ and $[w]^+$ ions for Pro, and relatively intense $[a]^+$ ions for aromatic residues (Tyr and Phe). We suggest that $[y_m + 2H]^+$ ions are produced from transient radical ions $[z_{m+1} + H]^{\cdot+}$.

1. Introduction

The importance of radical-driven dissociation (RDD) has long been recognized in the structural elucidation of organic compounds using mass spectrometry (MS) because of the specific cleavage initiated by a radical (unpaired electron) site [1]. Recent RDD researches on peptides and proteins utilize electron-capture dissociation (ECD) [2], electron-transfer dissociation (ETD) [3], ultraviolet photo-dissociation (UVPD) [4–7], and in-source decay (ISD) [8–10] combined with matrix-assisted laser desorption/ionization (MALDI) [11,12] and electrospray ionization (ESI) [13,14]. Traditionally, RDD employs electron ionization (EI) to form radical cations $[M]^{\cdot+}$ of volatile compounds. In modern RDD, the peptide radical ions can be generated by electron attachment to protonated analytes $[M+nH]^{n+}$ [2,3], short wavelength UV photon irradiation to analyte ions [4–6], and hydrogen atom binding to carbonyl oxygens of peptide backbones [9]. The structures of hydrogen-abundant protonated and hydrogen-deficient peptides $[M \pm H + H]^{\cdot+}$ are shown in Scheme 1a. RDD of peptides characteristically give amino (N)-terminal $[a]^+$, $[c + 2H]^+$, and $[d]^+$ ions and carboxyl (C)-terminal $[x]^+$, $[z + 2H]^+$, and $[w]^+$ ions [2,9,10]. In contrast, conventional low-energy collision-induced dissociation (low-E CID) of peptides results in $[b]^+$ and $[y + 2H]^+$ ions [15]. Herein we use the peptide fragment ion nomenclature proposed by Chu et al. [16] based on Biemann's nomenclature [17] (Scheme 1b).

In UVPD experiments, photo-induced homolytic cleavage of peptides at the Cα-C bond and consecutive RDD reactions can explain the formation of N-terminal $[a]^+$ and $[d]^+$ ions and C-terminal $[x]^+$ and $[w]^+$ ions. The mechanism is attributable to the Norrish type I photochemical reaction [5,18] (Scheme 2). However, it is likely that $[a]^+$ ions preferentially form from β-carbon (Cβ)-centered hydrogen-deficient peptide radical ions $[M - H\beta + H]^{\cdot+}$ [19–22]. Indeed, we also recently reported that $[a]^+$ ions are produced from the (Cβ)-centered radical ions $[M - H\beta + H]^{\cdot+}$ when MALDI-ISD is performed with a hydrogen-abstracting matrix 4-nitro-1-naphthol (4,1-NNL) [23] (Scheme 3). The Brodbelt group pointed out that $[a]^+$ ions generated by UVPD are useful for characterizing hydrogen-bonding motifs of proteins [24]. In UVPD, product ions originating from residue-specific cleavages at aromatic side chains, backbone C=O chromophore [22,25,26], at acidic Asp/Glu/Cys, and Pro effects in low-E CID [15] give structural information. Therefore, it is important to examine residue-specific cleavage of peptides from the standpoint of radical-driven dissociation (RDD).

Here, we examine the residue-specific cleavage of peptides containing Arg, Tyr, Phe, Asp, Pro, deuterated-Gly, and deuterated-

* Corresponding author.
E-mail address: takayama@yokohama-cu.ac.jp (M. Takayama).

https://doi.org/10.1016/j.ijms.2018.11.002
1387-3806/

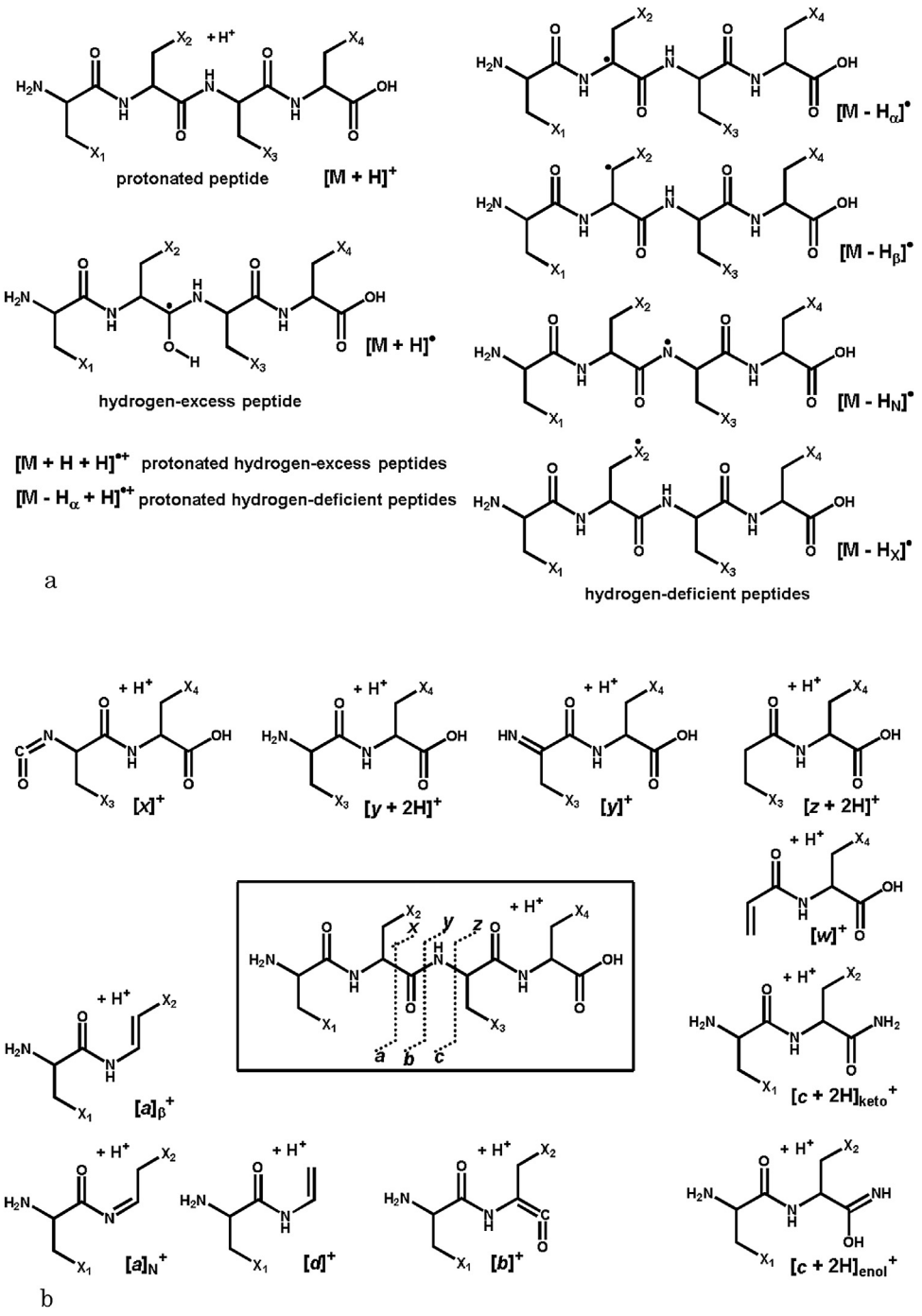

Scheme 1. a. Nomenclature of protonated peptide and hydrogen-excess/deficient peptides. b. Nomenclature of peptide product ions [16,17].

Ala residues using MALDI-ISD. The radical species, such as hydrogen-abundant and -deficient peptide ions, $[M \pm H + H]^{\cdot +}$, were generated with hydrogen-donating matrices 5-amino-1-naphthol (5,1-ANL) and 2,5-dihydroxybenzoic acid (2,5-DHB) and, hydrogen-abstracting matrices 4,1-NNL and 5-aminosalicylic acid (5-NSA), respectively. We also discuss the formation mechanisms of the product ions, especially $[y]^+$ and $[y + 2\,H]^+$ ions, in the different plume conditions and consecutive radical-driven dissociations of transient radical species.

2. Experimental

2.1. Materials

Matrix materials 5,1-ANL, 2,5-DHB, 4,1-NNL, and 5-NSA were purchased from Tokyo Chemical Industry (Tokyo, Japan). Synthetic peptides RGV-*d*5 (RGVKVDYG(d2)PAMAFA(d3)PADLAAEF, *M*r 2301.6) and EGV-*d*5 (EGVKVDYG(d2)PAMAFA(d3)PADLAARF, *M*r 2301.6) were obtained from Peptide Institute (Minoh, Osaka, Japan). Acetonitrile was purchased from Wako Pure Chemicals

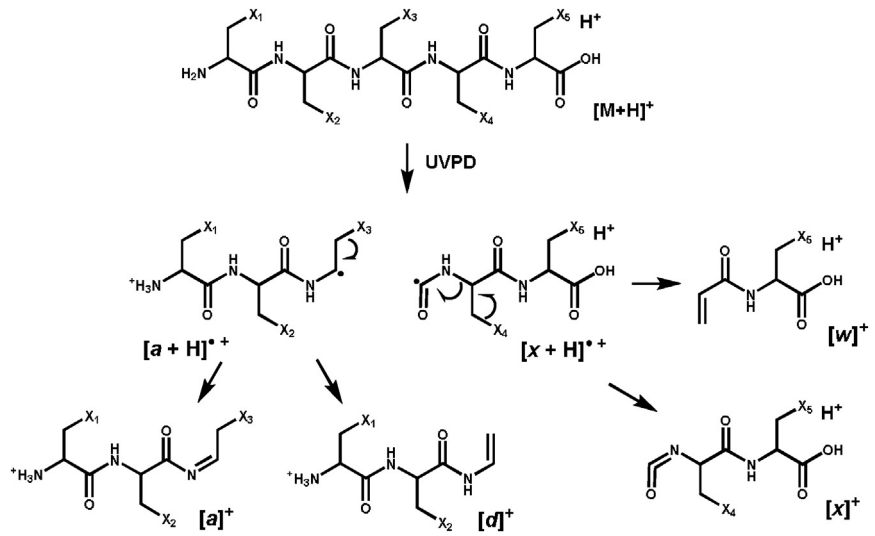

Scheme 2. The mechanism for the formation of $[a]^+$, $[d]^+$, $[x]^+$ and $[w]^+$ ions proposed from UVPD experiments of peptides [4–7,18–22].

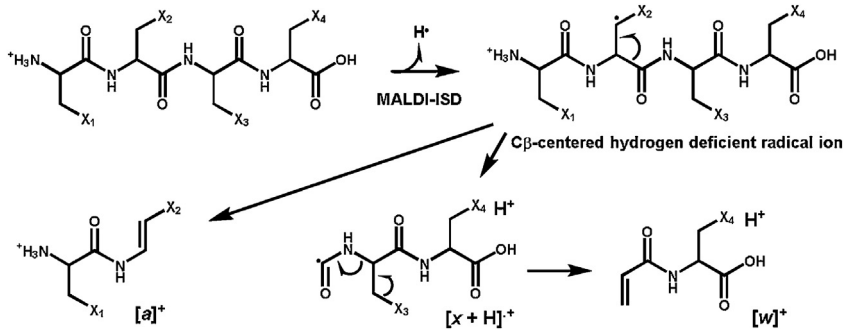

Scheme 3. The mechanism for the formation of $[a]^+$ and $[w]^+$ ions proposed from MALDI-ISD experiments of peptides with hydrogen-abstracting matrix [23].

(Osaka, Japan). Water used in all experiments was purified using a MilliQ water purification system from Millipore (Billerica, MA, USA). All reagents were used without further purification.

2.2. Mass spectrometry

MALDI-ISD experiments were performed with a time-of-flight mass spectrometer AXIMA-CFR (Shimadzu, Kyoto, Japan) equipped with a nitrogen laser (337 nm wavelength, 4 ns pulse width) operating at a pulse rate of 10 Hz. The laser spot size on the target substrate was *ca.* 100 μm in diameter. The ions generated by MALDI were accelerated using 20 kV with delayed extraction. The analyzer was operated in reflectron mode, and ions were detected using a microchannel plate detector. A total of 500 shots were accumulated for each mass spectrum acquisition.

2.3. Sample preparation

Analyte peptide was dissolved in water at a concentration of 100 pmol/μL. The matrix material was dissolved in water/acetonitrile (1:1, v/v) without any additives and the matrix solution was prepared at 10 mg/mL. A sample solution was prepared by mixing 10 μL of the dissolved analyte with 10 μL of matrix solution. A volume of 1.0 μL of the sample solution was deposited onto a stainless-steel MALDI plate, and the solvents were removed by evaporation in air at room temperature.

3. Results and discussion

3.1. Specific peptide fragment ions are generated in MALDI-ISD acquired with hydrogen-donating matrix

Positive-ion MALDI-ISD spectra of peptide RGV-*d*5 with an N-terminal Arg obtained with hydrogen-donating matrices 5,1-ANL and 2,5-DHB are shown in Fig. 1. The ISD spectrum acquired with 5,1-ANL only contained N-terminal $[c + 2\,H]^+$ ions except for $[c8 + 2\,H]^+$ and $[c14 + 2\,H]^+$ ions owing to the presence of Pro9 and Pro15 residues (Fig. 1a). The spectrum with 2,5-DHB showed preferential formation of $[c + 2\,H]^+$ ions and weak $[a]^+$ and $[y + 2\,H]^+$ ions, and some $[b]^+$ and $[d]^+$ ions (Fig. 1b). The ISD spectra of peptide EGV-*d*5 with a C-terminal Arg obtained with 5,1-ANL and 2,5-DHB are shown in Fig. 2. In contrast to the RGV-d5 spectrum with 5,1-ANL, the ISD spectrum of EGV-*d5* mainly yielded $[z + 2\,H]^+$ product ions. The ions, $[z8 + 2\,H]^+$ and $[z14 + 2\,H]^+$, were not observed due to the presence of Pro9 and Pro15 residues (Fig. 2a). This spectrum also has $[c + 2\,H]^+$, $[z\text{-matrix} + H]^+$ and $[y + 2\,H]^+$ ions. Interestingly, when 5,1-ANL was employed, the intensity of $[y16 + 2\,H]^+$ ion originating from cleavage at the C–N bond of Asp6-Tyr7 residues was higher than that of $[z16 + 2\,H]^+$, while the intensity of $[z_n + 2\,H]^+$ ions was more intense than that of the corresponding $[y_n + 2\,H]^+$ ions (Fig. 2a). In contrast, the ISD spectrum with 2,5-DHB demonstrated preferential production of $[y + 2\,H]^+$ rather than $[z + 2\,H]^+$ ions (Fig. 2b). It is noteworthy that $[z + 2\,H]^+$ ions were not observed due to the lack of strong protonation sites in z-fragments (Fig. 1b), whereas both Fig. 2a and b showed the C-terminal pair of $[y + 2\,H]^+$ and $[z + 2\,H]^+$ ions because of the presence of an Arg residue.

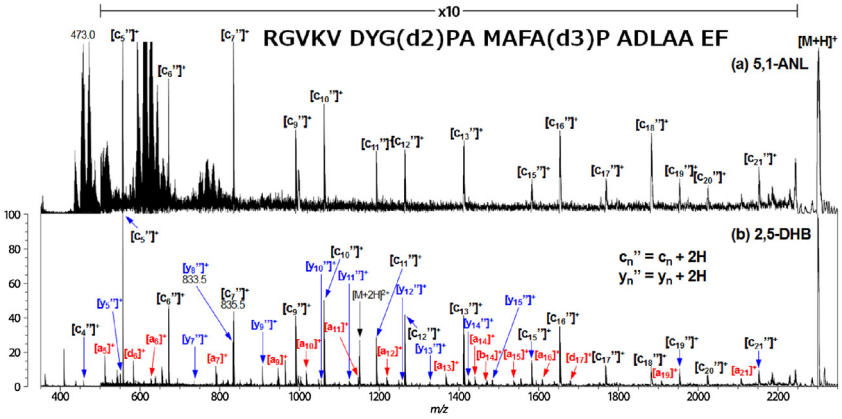

Fig. 1. MALDI-ISD spectra of peptide RGV-*d*5 containing an N-terminal Arg obtained with hydrogen-donating matrices (a) 5-amino-1-naphthol (5,1-ANL) and (b) 2,5-dihydroxylbenzoic acid (2,5-DHB).

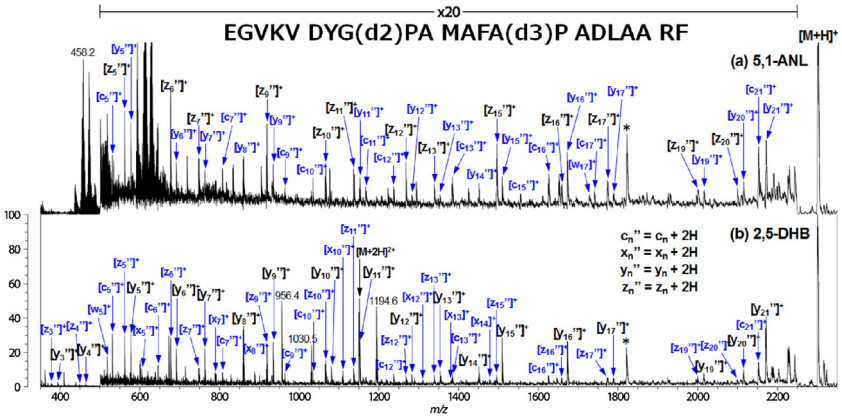

Fig. 2. MALDI-ISD spectra of peptide EGV-*d*5 containing a C-terminal Arg obtained with hydrogen-donating matrices (a) 5-amino-1-naphthol (5,1-ANL) and (b) 2,5-dihydroxylbenzoic acid (2,5-DHB).

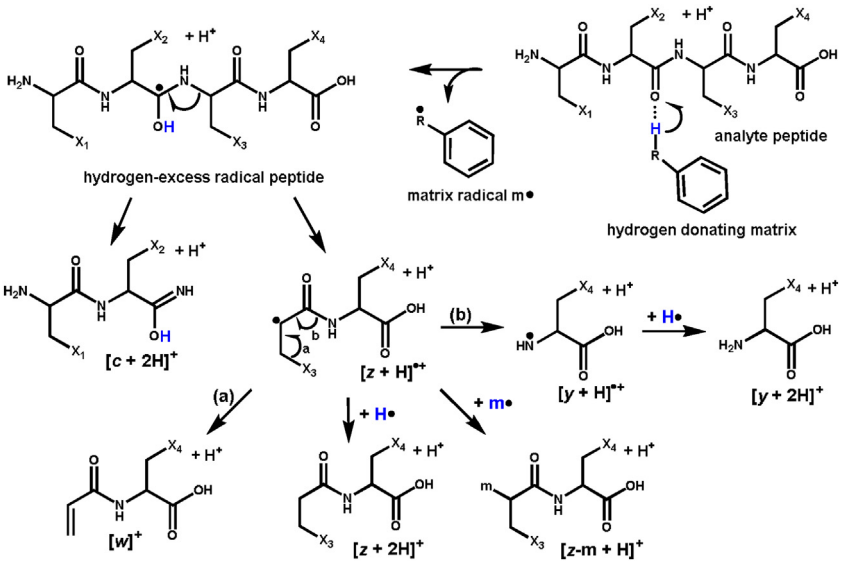

Scheme 4. Proposed MALDI-ISD mechanism of peptides with hydrogen-donating matrix.

The MALDI-ISD mechanism of peptides and proteins with hydrogen-donating matrix can be explained by a prompt (within several tens ns) and specific cleavage at the N-Cα bond of the peptide backbone. It results from the generation of hypervalent radical species such as carbonyl-carbon (C_{CO})-centered hydrogen-abundant radical peptides and proteins [M + H_{CO}]· (Scheme 4). In MALDI-ISD experiments, the prompt and specific cleavage takes place independently of ionization (protonation and deprotonation) [27,28]. The C_{CO}-centered hydrogen-abundant radical peptides and proteins [M + H_{CO}]· are formed *via* hydrogen transfer from phe-

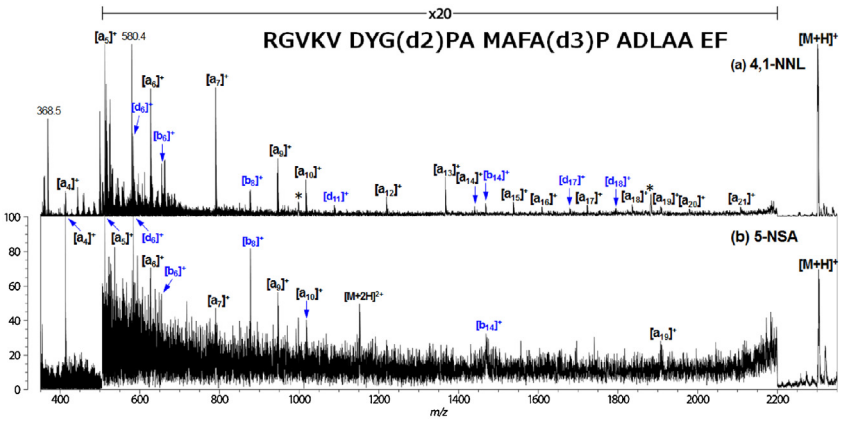

Fig. 3. MALDI-ISD spectra of RGV-*d5* with hydrogen-abstracting matrices (a) 4-nitro-1-naphthol (4,1-NNL) and (b) 5-nitro-salycylic acid (5-NSA). The asterisk indicates a metastable peak.

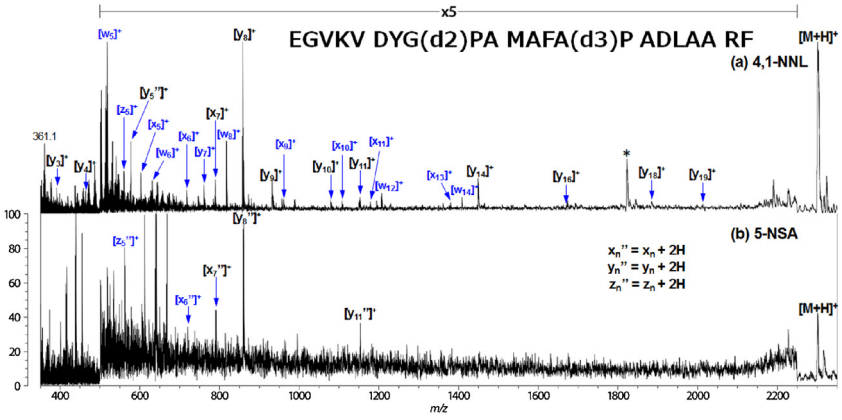

Fig. 4. MALDI-ISD spectra of EGV-*d5* with hydrogen-abstracting matrices (a) 4-nitro-1-naphthol (4,1-NNL) and (b) 5-nitro-salycylic acid (5-NSA). The asterisk indicates a metastable peak.

nolic (Ph−OH) and anilinic (Ph-NH_2) matrix active hydrogens to the carbonyl oxygens of backbone by intermolecular hydrogen-bonding [9]. The salient characteristic of positive-ion ISD spectra of peptides is the production of N-terminal $[c + 2H]^+$ ions. In contrast, C-terminal $[z + 2H]^+$ and $[z\text{-}m + H]^+$ ions are formed by hydrogen H·and matrix radicals m·binding to transient radical species $[z + H]^{\cdot+}$ in MALDI plumes [29,30], as depicted in Scheme 4. Although the formation of $[c + 2H]^+$, $[z + 2H]^+$, and $[z\text{-}m + H]^+$ ions observed in Figs. 1a and 2 a can be rationalized by radical-initiated reactions shown in Scheme 4, the detailed mechanism for the formation of $[y + 2H]^+$ ions is not yet clear. A possible mechanism of $[y + 2H]^+$ ion formation may be hydrogen attachment to transient radical ions $[y + H]^{\cdot+}$ (Scheme 4), as described in section 3.3.

The ISD spectra of RGV-*d5* and EGV-*d5* obtained with 2,5-DHB differ from those acquired with 5,1-ANL (Figs. 1 and 2b). The ISD spectrum of RGV-*d5* showed C-terminal $[y + 2H]^+$ ions but no $[z + 2H]^+$ and $[z\text{-}m + H]^+$ ions, while that of EGV-*d5* contained $[y + 2H]^+$, $[z + 2H]^+$, and $[z\text{-}m + H]^+$ ions. The lack of $[z + 2H]^+$ and $[z\text{-}m + H]^+$ ions in Fig. 1b may be due to the absence of an NH_2 group or Arg residue in those fragments (Scheme 4). In contrast, the ISD spectra of EGV-*d5* clearly showed $[z + 2H]^+$ and $[z\text{-}m + H]^+$ ions because an Arg residue is located on the C-terminus (Fig. 2b). The formation of $[a]^+$, $[d]^+$, and $[x + 2H]^+$ ions observed in the ISD spectra of RGV-*d5* and EGV-*d5* ions obtained with 2,5-DHB (Figs. 1 and 2b) are described in next section.

3.2. Specific peptide fragment ions are generated in MALDI-ISD with hydrogen-abstracting matrix

The MALDI-ISD spectra of peptide RGV-*d5* obtained with hydrogen-abstracting matrices 4,1-NNL and 5-NSA are shown in Fig. 3. The ISD spectrum with 4,1-NNL mainly showed N-terminal $[a]^+$ ions, except for $[a8]^+$ and $[a11]^+$ ions arising from cleavage at the Cα-C bond of Gly8-Pro9 and Met11-Ala12 residues, respectively (Fig. 3a). The spectrum with 5-NSA also contained some $[a]^+$ and $[b]^+$ ions (Fig. 3b). In Fig. 3a, it should be noted that $[a7]^+$ and $[a13]^+$ ions originating from cleavage at the Cα-C bond of aromatic side chains Tyr7-Gly8 and Phe13-Ala14 residues have a significantly high intensity. On the other hand, ISD of EGV-*d5* with 4,1-NNL mainly yielded $[y]^+$, $[x]^+$ and $[w]^+$ ions. Particularly noteworthy are the high intensities of $[y8]^+$ and $[y14]^+$ ion peaks that originate from cleavage at the C–N bond of Xxx-Pro residues (Fig. 4a). Conversely, the spectrum acquired with 5-NSA only resulted in few $[y + 2H]^+$ and $[x + 2H]^+$ ions (Fig. 4b). The mechanism of MALDI-ISD with hydrogen-abstracting matrix can be rationalized by the RDD reactions of the β-carbon (Cβ)-centered radical peptide ions $[M - Hβ + H]^{\cdot+}$, as shown in Scheme 5 [23]. The RDD reactions of Scheme 5 can also explain the lack of $[a]^+$ ions arising from the cleavage of Gly-Xxx residues.

The matrix effect on the ISD spectrum of EGV-*d5* is of significant interest. The ISD spectrum of this peptide obtained with 4,1-NNL contains C-terminal $[x]^+$, $[y]^+$ and $[z]^+$ ions (Fig. 4a), whereas the

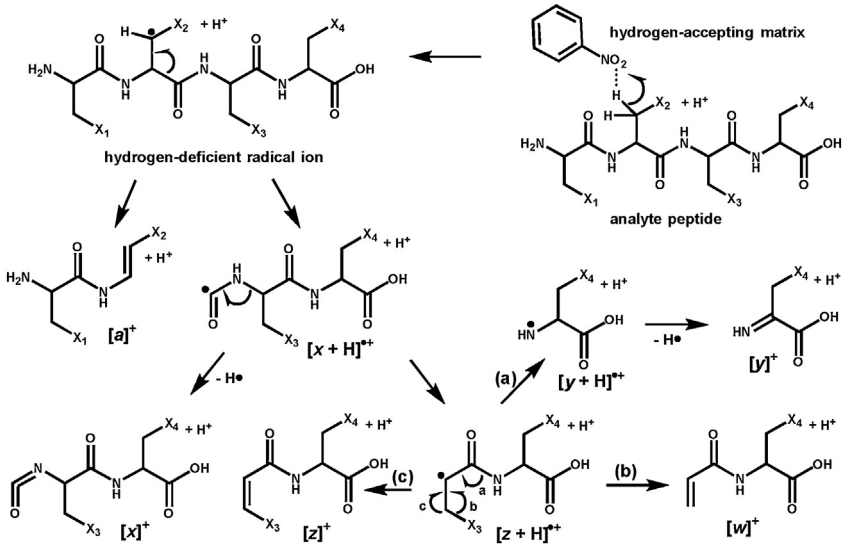

Scheme 5. MALDI-ISD mechanism of peptides with hydrogen-abstracting matrix.

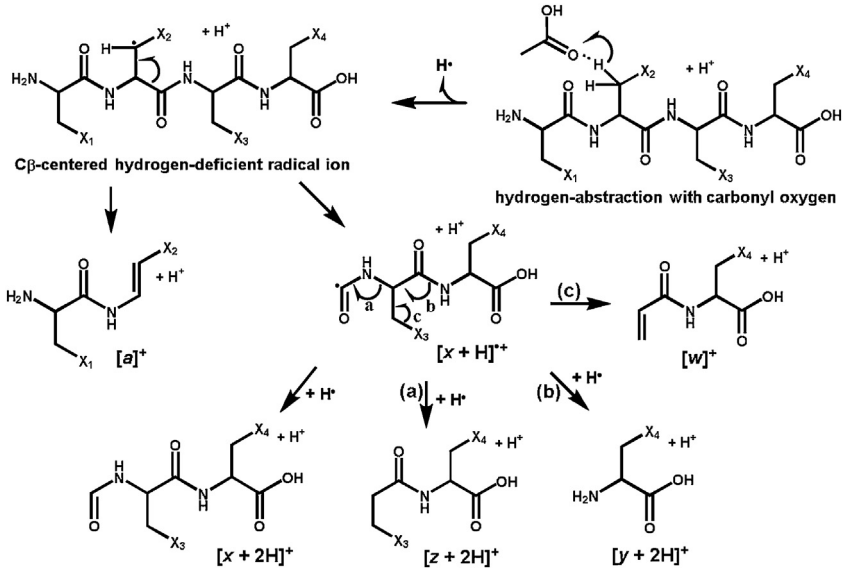

Scheme 6. MALDI-ISD reactions in the plume with 2,5-DHB matrix.

spectrum acquired with 2,5-DHB had $[x+2\,H]^+$, $[y+2\,H]^+$, and $[z+2\,H]^+$ ions (Fig. 2b). Use of the hydrogen-abstracting matrix 4,1-NNL may form a dense gas-like MALDI plume devoid of hydrogen radicals H. Conversely, hydrogen-donating matrices 5,1-ANL and 2,5-DHB form a MALDI plume abundant in hydrogen and matrix radicals (H· and m·). In fact, $[c+2\,H]^+$, $[x+2\,H]^+$, $[y+2\,H]^+$, $[z+2\,H]^+$ and $[w]^+$ fragment ions observed in the ISD spectra of RGV-*d5* and EGV-*d5* with 5,1-ANL can be perfectly rationalized by the binding processes of hydrogen and matrix radicals (H· and m·) with the transient radical species $[z+H]^{\cdot+}$ and $[y+H]^{\cdot+}$ (Scheme 4). In contrast, the fragment ions $[a]^+$, $[x]^+$, $[y]^+$, $[z]^+$, and $[w]^+$ were observed in the ISD spectra acquired with hydrogen-abstracting matrix 4,1-NNL, (Figs. 3 and 4a). This observation can be explained by the loss of hydrogen from the transient radicals $[x+H]^{\cdot+}$ and $[y+H]^{\cdot+}$ (Scheme 5) that may occur in plumes lacking hydrogen radicals.

Regarding the ISD spectrum of EGV-*d5* with 2,5-DHB (Fig. 2b), it should be noted that this matrix has both hydrogen-donating and -abstracting properties, due to the presence of phenolic hydroxyl (Ph−OH) and carboxyl carbonyl (COOH) groups, respectively. The presence of a carbonyl oxygen in MALDI matrix results in $[a]^+$ ions, as well as $[c+2\,H]^+$, $[y+2\,H]^+$, and $[z+2\,H]^+$ ions [31]. Therefore, the $[a]^+$, $[x+2\,H]^+$, $[y+2\,H]^+$, $[z+2\,H]^+$, and $[w]^+$ fragment ions observed in the ISD spectra of RGV-*d5* (Fig. 1b) and EGV-*d5* (Fig. 2b) obtained with 2,5-DHB can be explained by the formation of the Cβ-centered hydrogen-deficient radical ions $[M-H_\beta+H]^{\cdot+}$ and subsequent RDD reactions leading to $[a]^+$ and $[x+H]^+$ ions (Scheme 6). The resulting transient radical ions $[x+H]^{\cdot+}$ may produce $[x+2\,H]^+$, $[y+2\,H]^+$, and $[z+2\,H]^+$ ions *via* hydrogen binding in the hydrogen atom rich plume.

3.3. $[Y_m+2\,H]^+$ ions are produced from $[z_{m+1}+H]^{\cdot+}$ radical ions

When hydrogen-donating matrices 5,1-ANL and 2,5-DHB were used, the ISD spectra of EGV-*d5* showed preferential production of C-terminal $[z+2\,H]^+$ and $[y+2\,H]^+$ ions (Fig. 2), respectively. Although the formation of $[z+2\,H]^+$ ions (and also $[z\text{-}m+H]^+$) can be explained by binding of hydrogen H·and matrix radical m·to the transient radical ions $[z+H]^{\cdot+}$ in MALDI plumes (Scheme 4)

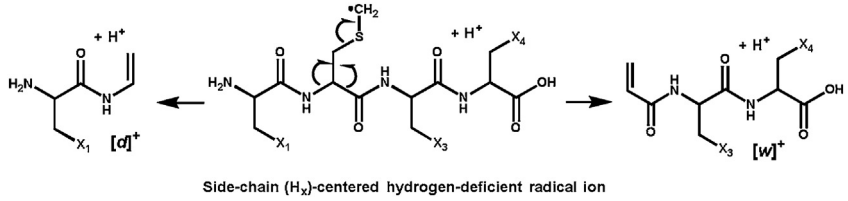

Scheme 7. xxx.

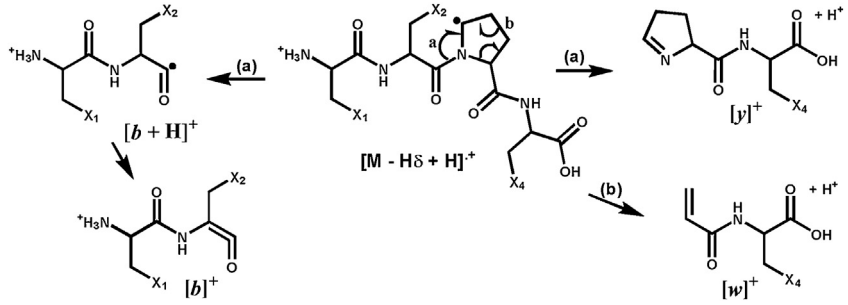

Scheme 8. xxx.

[29,30], the mechanism of $[y + 2\,H]^+$ ion production has not previously been described. Interestingly, the ISD spectrum of EGV-*d5* gave a relatively intense peak corresponding to $[y16 + 2\,H]^+$ ion originating from cleavage at the C–N bond of Asp6-Tyr7 residues, while other $[y_m + 2\,H]^+$ ion intensities were lower than $[z_m + 2\,H]^+$ ions (Fig. 2a). The reason why the intensity of the $[y16 + 2\,H]^+$ ion is high may be because the ISD fragments $[c + 2\,H]^+$ originating from cleavage at the N-Cα bond of Xxx-Asp residues of peptides and proteins give rise to discontinuous intense peaks [32]. In fact, the $[c5 + 2\,H]^+$ and $[c16 + 2\,H]^+$ ions originating from the cleavage of Xxx-Asp yield non-sequential intense peaks compared to the other $[c + 2\,H]^+$ ions (Fig. 1). According to the specific N-Cα bond cleavage (Scheme 3) as for Val5-Asp6, the relatively abundant radical ion $[z17 + H]^{\cdot+}$ is formed as a pair of abundant $[c5 + 2\,H]^+$ ion in Fig. 1. The resulting $[z17 + H]^{\cdot+}$ ion may occur by consecutive radical-driven dissociation (RDD) leading to the formation of the transient radical ion species $[y16 + H]^{\cdot+}$. However, these transient radical ions could not be observed in the ISD spectra. Similar consecutive RDD reactions have been reported in a study on the cascade dissociation of peptide-radical cations $[z + H]^{\cdot+}$ [33]. Therefore, the $[y16 + 2\,H]^+$ ion could be formed by binding hydrogen to the radical y-ion $[y16 + H]^{\cdot+}$ resulting from the transient radical z-ion $[z17 + H]^{\cdot+}$. Therefore, the most likely mechanism of $[y_{m-1} + 2\,H]^+$ formation in Fig. 2a can be explained by the competitive reactions of the $[z_m + H]^{\cdot+}$ ions, as shown in Scheme 4.

3.4. Residue-specific dissociation in MALDI-ISD

In the ISD spectra of the analyzed peptides, specific cleavage was observed at Asp, Met, Pro, Phe, and Tyr residues. The $[d6]^+$ and $[d17]^+$ ions originating from cleavage at both Cα-C and Cβ-Cδ bonds of Asp-Xxx residues were detected (Figs. 1b and 3). The Asp effect on $[d]^+$ ion formation also occurs in ultraviolet photodissociation (UVPD) of peptides [34] as shown in Scheme 2. The specific effects of Asp on protein cleavage have also been observed at the N-Cα bond cleavage of Xxx-Asp in MALDI-ISD [32] and selective/enhanced cleavage at the C–N bond of Asp-Xxx residues in low-energy CID [15,35]. The residue effect on the formation of $[d]^+$ ions was also observed at the cleavage of both N-Cα and Cβ-Cδ bonds of Met-Xxx residues (Fig. 3a). The $[w12]^+$ fragment ion was formed as a consequence of the presence of Met (Fig. 4a). The effect of this amino acid results in side-chain loss without the observation of $[a11]^+$ and $[y12]^+$ ions possibly due to the loss of hydrogen from the side-chain methyl group (Scheme 7). The characteristic peaks corresponding to $[b8]^+$ and $[b14]^+$ ions in Fig. 3a and $[y8]^+$, $[y14]^+$, $[w8]^+$, and $[w14]^+$ ions in Fig. 4a may be due to a Pro effect. RDD reactions of the δ-carbon (Cδ)-centered radical peptide ions $[M-H\delta + H]^{\cdot+}$ can explain how this effect may occur (Scheme 8) [23]. Regarding $[a]^+$ ion formation, cleavage at the Cα-C bond of the Tyr-Xxx and Phe-Xxx residues gave relatively intense $[a7]^+$ and $[a13]^+$ ions peaks (Fig. 3a). This aromatic residue effect is a characteristic of UVPD of peptides and proteins [22,25,26]. As described above, it should be recognized that the specific cleavage of hydrogen-deficient peptide ions $[M-H + H]^{\cdot+}$ strongly depends upon the amino acid residues and the sites of a radical (unpaired electron).

4. Conclusions

The peptide fragment ion types observed in MALDI-ISD spectra obtained with hydrogen-donating and -abstracting matrix can be explained by the radical-driven dissociation (RDD) of the hydrogen-abundant/deficient radical ions $[M \pm H + H]^{\cdot+}$. The ISD spectrum of EGV-*d5* acquired with a hydrogen-abstracting matrix 4,1-NNL showed C-terminal $[x]^+$, $[y]^+$ and $[z]^+$ ions, while the spectrum obtained with a hydrogen-donating matrices 5,1-ANL and 2,5-DHB contained $[x + 2\,H]^+$, $[y + 2\,H]^+$ and $[z + 2\,H]^+$ ions, depending upon the MALDI plume deficient or rich in hydrogen radicals $H^{\cdot}$. The ISD experiments with 4,1-NNL mainly resulted in $[a]^+$, $[x]^+$, $[y]^+$ and $[w]^+$ ions, explained by the RDD $[M - H\beta + H]^{\cdot+}$ radical ions, whereas the spectra with 5,1-ANL typically showed $[c + 2\,H]^+$ and $[z + 2\,H]^+$ ions. The ISD spectra obtained with hydrogen-abstracting matrix specifically had $[a]^+$, $[b]^+$, $[d]^+$, $[y]^+$ and $[w]^+$ ions, but this depended upon the presence of Asp, Met, Pro, Phe and Tyr residues. We suggest that $[y_m + 2\,H]^+$ ions are produced from transient radical ions $[z_{m+1} + H]^{\cdot+}$.

Acknowledgements

MT gratefully acknowledges the support from the Creation of Innovation Centers for Advanced Interdisciplinary Research Area Program in the Special Coordination Fund for Promoting Science and Technology, and the Grant-in-Aid for Scientific Research (C)

(15K05545) from the Japan Ministry of Education, Culture, Sports and Technology.

References

[1] F.W. McLafferty, F. Turecek, Interpretation of Mass Spectra, 4th ed., University Science Books, CA, USA, 1993.
[2] R.F. Zubarev, N.L. Kelleher, F.W. McLafferty, Electron capture dissociation of multiply charged protein cations. A nonergodic process, J. Am. Chem. Soc. 120 (1988) 3265–3266.
[3] J.E.P. Syka, J.J. Coon, M.J. Schroeder, J. Shabanowitz, D.F. Hunt, Peptide and protein sequence analysis by electron transfer dissociation mass spectrometry, Proc. Natl. Acad. Sci. U. S. A. 101 (2004) 9528–9533.
[4] M.S. Thompson, W. Cui, J.P. Reilly, Fragmentation of singly charged peptide ions by photodissociation at λ=157 nm, Angew. Chem. Int. Ed. 43 (2004) 4791–4794.
[5] W. Cui, M.S. Thompson, J.P. Reilly, Pathways of peptide ion fragmentation induced by vacuum ultraviolet light, J. Am. Soc. Mass Spectrom. 16 (2005) 1384–1398.
[6] J.A. Madsen, R.R. Cheng, T.S. Kaoud, K.N. Dalby, D.E. Makarov, J.S. Brodbelt, Charge-site dependent dissociation of hydrogen-rich radical peptide cations upon vacuum UV photoexcitation, Chemistry 18 (2012) 5374–5383.
[7] F. Turecek, Peptide radicals and cation radicals in the gas phase, Chem. Rev. 113 (2013) 6691–6733.
[8] R.S. Brown, J.J. Lennon, Sequence-specific fragmentation of matrix-assisted laser-desorbed protein/peptide ions, Anal. Chem. 67 (1995) 3990–3999.
[9] M. Takayama, N-Cα bond cleavage of the peptide backbone via hydrogen abstraction, J. Am. Soc. Mass Spectrom. 12 (2001) 1044–1049.
[10] J. Hardouin, Protein sequence information by matrix-assisted laser desorption/ionization in-source decay mass spectrometry, Mass Spectrom. Rev. 26 (2007) 672–682.
[11] M. Karas, D. Bachmann, U. Bahr, F. Hillenkamp, Matrix-assisted ultraviolet laser desorption of non-volatile compounds, Int. J. Mass Spectrom. Ion Proc. 78 (1987) 53–68.
[12] K. Tanaka, H. Waki, Y. Ido, S. Akita, Y. Yoshida, T. Yoshida, Protein and polymer analyses up to m/z 100000 by laser ionization time-of-flight mass spectrometry, Rapid Commun. Mass Spectrom. 2 (1988) 151–153.
[13] C.M. Whitehouse, R.N. Dreyer, M. Yamashita, J.B. Fenn, Electrospray interface for liquid chromatographs and mass spectrometers, Anal. Chem. 57 (1985) 675–679.
[14] J.B. Fenn, M. Mann, C.K. Meng, S.F. Wong, C.M. Whitehouse, Electrospray ionization for mass spectrometry of large biomolecules, Science 46 (1989) 64–71.
[15] B. Paizs, S. Suhai, Fragmentation pathways of protonated peptides, Mass Spectrom. Rev. 24 (2005) 508–548.
[16] I.K. Chu, J.C.-K. Siu, J.K.-C. Lau, W.K. Tang, X. Mu, C.-K. Lai, X. Guo, X. Wang, N. Li, Y. Xia, X. Kong, H.B. Oh, V. Ryzhov, F. Turecek, A.C. Hopkinson, Proposed nomenclature for peptide ion fragmentation, Int. J. Mass Spectrom. 390 (2015) 24–27.
[17] K. Biemann, Contributions of mass spectrometry to peptide and protein structure, Biomed. Environ. Mass Spectrom. 16 (1988) 99–111.
[18] F. Canon, A.R. Milosavljevic, L. Nahon, A. Giuliani, Action spectroscopy of a protonated peptide in the ultraviolet range, Phys. Chem. Chem. Phys. 17 (2015) 25725–25733.
[19] J. Laskin, Z. Yang, C. Lam, I.K. Chu, Charge-remote fragmentation of odd-electron peptide ions, Anal. Chem. 79 (2007) 6607–6614.
[20] L. Zhang, J.P. Reilly, Radical-driven dissociation of odd-electron peptide radical ions produced in 157 nm photodissociation, J. Am. Soc. Mass Spectrom. 20 (2009) 1378–1390.
[21] J.P. Reilly, Ultraviolet photofragmentation of biomolecular ions, Mass Spectrom. Rev. 28 (2009) 425–447.
[22] M. Xu, T. Song, Q. Quan, Q. Hao, D.-C. Fang, C.-K. Siu, I.K. Chu, Effect of the N-terminal basic residue on facile Cα-C bond cleavages of aromatic-containing peptide radical cations, Phys. Chem. Chem. Phys. 13 (2011) 5888–5896.
[23] K. Nagoshi, M. Yamakoshi, K. Sakamoto, M. Takayama, Specific Cα-C bond cleavage of β-carbon-centered radical peptides produced by matrix-assisted laser desorption/ionization mass spectrometry, J. Am. Soc. Mass Spectrom. 29 (2018) 1473–1483.
[24] L.J. Morrison, W. Chai, J.A. Rosenberg, G. Henkelman, J.S. Brodbelt, Characterization of hydrogen bonding motifs in proteins: hydrogen elimination monitoring by ultraviolet photodissociation mass spectrometry, Phys. Chem. Chem. Phys. 19 (2017) 20057–20074.
[25] T. Ly, R.R. Julian, Residue-specific radical-directed dissociation of whole proteins in the gas phase, J. Am. Chem. Soc. 130 (2008) 351–358.
[26] X. Mu, T. Song, M. Xu, C.-K. Lai, C.-K. Siu, J. Laskin, I.K. Chu, Discovery and mechanistic studies of facile N-terminal Cα-C bond cleavages in the dissociation of tyrosine-containing peptide radical cations, J. Phys. Chem. B 118 (2014) 4273–4281.
[27] M. Takayama, A. Tsugita, Does in-source decay occur independent of the ionization process in matrix-assisted laser desorption? Int. J. Mass Spectrom. 181 (1998) L1–L6.
[28] M. Takayama, A. Tsugita, Sequence information of peptides and proteins with in-source decay in matrix-assisted laser desorption/ionization time-of-flight mass spectrometry, Electrophoresis 21 (2000) 1670–1677.
[29] T. Koecher, A. Engstroem, R.A. Zubarev, Fragmentation of peptides in MALDI in-source decay mediated by hydrogen radicals, Anal. Chem. 77 (2005) 172–177.
[30] K. Demeure, L. Quinton, V. Gabelica, E. de Pauw, Rational selection of the optimum MALDI matrix for top-down proteomics by in-source decay, Anal. Chem. 79 (2007) 8678–8686.
[31] M. Takayama, In-source decay characteristics of peptides in matrix-assisted laser desorption/ionization time-of-flight mass spectrometry, J. Am. Soc. Mass Spectrom. 12 (2001) 420–427.
[32] M. Takayama, K. Nagoshi, R. Iimuro, K. Inatomi, Access of hydrogen-radicals to the peptide-backbone as a measure for estimating the flexibility of proteins using matrix-assisted laser desorption/ionization mass spectrometry, Int. J. Mol. Sci. 15 (2014) 8428–8442.
[33] T.W. Chung, R. Hui, A. Ledvina, J.J. Coon, F. Turecek, Cascade dissociation of peptides cation-radicals. Part 1. Scope and effects of amino acid residues in penta-, nona-, and decapeptides, J. Am. Soc. Mass Spectrom. 23 (2012) 1336–1350.
[34] N. DeGraan-Weber, S.A. Ward, J.P. Reilly, A novel triethylphosphonium charge tag on peptides, derivatization, and fragmentation, J. Am. Soc. Mass Spectrom. 28 (2017) 1889–1900.
[35] C. Gu, G. Tsaprailis, L. Breci, V.H. Wysocki, Selective gas-phase cleavage at the peptide bond C-terminal to aspartic acid in fixed-charge derivatives of Asp-containing peptides, Anal. Chem. 72 (2000) 5804–5813.